



## The Synthesis and Crystallization of Poly(vinylidene fluoride) in Supercritical CO<sub>2</sub>

Zhendong Shi,<sup>1,3</sup> Zhen Zheng,<sup>1</sup> Xiaoli Su,<sup>2</sup> Xinling Wang<sup>1\*</sup>

<sup>1</sup>College of Chemistry and Chemical Engineering, Shanghai Jiao Tong University, 800 Dongchuan Road, Shanghai 200240, P. R. China; Fax: +86-21-54741297; xlwang@sjtu.edu.cn, shizhd@sjtu.edu.cn, zzheng@sjtu.edu.cn

<sup>2</sup>Shanghai 3F New Materials Co., Ltd., 4411 LongWu Road, Shanghai 200241, P. R. China; Suxiaoli@sh3f.com

<sup>3</sup>School of Chemistry and life, Three Gorges University, 8 Daxue Road, Yichang 443000, Hubei Province, P. R. China

(Received: 3 August, 2006; published: 20 December, 2006)

**Abstract:** A series of poly(vinylidene fluoride)s (PVDFs) is synthesized in supercritical carbon dioxide (sc-CO<sub>2</sub>). The influences of polymerization pressure, molecular weight distribution and H-H defect concentration on the crystallization of PVDF have been studied in combination with differential scanning calorimetry (DSC), wide-angle X-ray diffraction (WAXRD) and Fourier transform infrared spectroscopy (FT-IR) measurements. The result shows that the morphology, molecular weights, polydispersity and head-to-head (H-H) defect concentrations of the PVDFs are affected by the reaction pressure and good solubility generated from sc-CO<sub>2</sub>. Especially, the sc-CO<sub>2</sub> polymerization has greatly improved the crystallization mode of the obtained PVDFs such as the complete degree of crystallinity, crystallinity and the crystal phase. This will create more comprehensive application fields for PVDF.

### Introduction

Much attention has been paid to poly(vinylidene fluoride) (PVDF) over years because of its excellent processability, superior mechanical characteristics, pyro-electric properties, good chemical and water resistant function, and extremely high fluidity in a wide range of working temperatures [1]. PVDF is known to be semicrystalline polymer with five different polymorphs, the so-called  $\alpha$ ,  $\beta$ ,  $\gamma$ ,  $\delta$ , and  $\epsilon$  forms [2].  $\beta$  phase has piezo- and pyro-properties [3]. This thermoplastic polymer has been widely used for pipes, valves, coatings, films, cables and pumps as well as a acceptable biomaterial [4].

Usually, PVDF is produced by either emulsion or suspension techniques, at monomer pressure between 10 and 200 bar and temperature from 10 to 130 °C [5, 6]. In both processes, large quantities of wastewater are generated and large quantities of energy are consumed to dry the polymer. Both polymerizations of PVDF often require stabilizers and surfactants which greatly increase the difficulty for purification of the final products. An environmentally friendly manufacturing process for PVDF would be more attractive if it could eliminate the generation of waste streams and reduce the need for polymer drying. The new technique will be really simple and relevant alternative if it can minimize the need of additives for polymerization.

Supercritical carbon dioxide polymerization is a promising technique to fulfill the requirements [7]. CO<sub>2</sub> is nontoxic, nonflammable, inexpensive, volatile and readily available. It can be easily separated from other components and has a readily accessible critical point ( $T_{cr}$  31.1 °C;  $P_{cr}$  73.8 bar). In addition, for both supercritical and liquid CO<sub>2</sub>, the dielectric constant varies from 1.2 to 1.5, and its viscosity is also low under both supercritical and liquid conditions [8]. All these advantages make the CO<sub>2</sub> an excellent reaction media for the polymerization [9]. Nowadays, polymerization in sc-CO<sub>2</sub> has drawn more and more attention due to its great advantages [10].

In the early 1990s, DeSimone first described homogeneous free radical polymerization of fluoropolymers in sc-CO<sub>2</sub> [11]. Then, they reported the continuous precipitation polymerization of vinylidene fluoride (VDF) in sc-CO<sub>2</sub> [12, 13]. They set up an extended homogeneous kinetic model predicting the polydispersities of PVDF reasonably well [10]. Very recently, Howdle et al. have studied the effects of stabilizers on dispersion polymerization of VDF in sc-CO<sub>2</sub> and obtained high molecular weight products with well-defined and uniform spherical particles [14-16]. However, the influence of sc-CO<sub>2</sub> on the crystallization behaviors of PVDF has never been investigated up to now.

So far, the crystallization of commercial PVDF (not by sc-CO<sub>2</sub> polymerization) under electric fields or high pressure or by heat treatments has been studied [17-23]. It is found that many factors, such as the temperature, H-H defect, electric fields, pressure, molecular weight and chain end groups, affect the crystalline phases ( $\alpha$ ,  $\beta$ , and  $\gamma$  phase), phase transition and crystallinity of PVDF [24- 26]. However, it will be interesting to study the effect of sc-CO<sub>2</sub> on the crystallization of PVDF.

This paper presents the polymerization of VDF in sc-CO<sub>2</sub>, as well as the investigation of the effects of the sc-CO<sub>2</sub> features, especially pressure, on polymer micro morphology, molecular sequence structure and crystalline behaviors. The sc-CO<sub>2</sub> polymerization is found to have great advantages in controlling the product micro morphology, molecular sequence structure, complete degree of crystallinity as well as the crystal phase.

## Results and Discussion

### *Polymerization of VDF in sc-CO<sub>2</sub>*

#### *-Effect of reaction conditions on molecular weight and polydispersity*

A series of sc-PVDFs were polymerized under different reaction pressures in sc-CO<sub>2</sub>. The results (Table 1) show that the molecular weight of PVDF increase with the decrease of initiator concentration, see sc-3, 4, 8 in Table 1, the molecular weight increase by about eight times from  $5.2 \times 10^4$  to  $39.7 \times 10^4$  g/mol when the initiator concentration decrease to a forth from 15.6 to 3.83 mmol/L, and their initial monomer concentrations are approximately equivalent. The influence of monomer concentration on molecular weight is contrary to the initiator concentration. The increase of molecular weight with the increasing monomer concentration is augmented to a surprise degree, partially due to the reaction pressure. See sc-1 and sc-2 in Table 1, the molecular weight and polydispersity increase from  $9.1 \times 10^4$  to  $40.5 \times 10^4$  and from 1.41 to 1.66, respectively, when the initial pressure increase from 10.5 to 26 MPa, although the monomer concentration only increase from 3.13 to 4.38 mol/L. Moreover, see sc-5 and sc-6, the polydispersity also increases from 1.79 to

2.01 when the initial pressure increases from 24.5 to 27.5 MPa.

The initial reaction pressure is an assignable influencing factor on polymer molecular weight and polydispersity. DeSimone and Howdle have reported independently that the increased reaction pressure increases the molecular weight and polydispersity of PVDF polymerized in sc-CO<sub>2</sub> by both the continuous process and the batch process [13, 27-28]. The reason might be proposed as following: the activation volume is negative during the polymerization reaction of VDF in sc-CO<sub>2</sub> according to the transition-state theory [29, 30]. The reaction proceeds at the direction of the reducing pressure, and the higher initial reaction pressure beneficially generates the more rapid initial reaction rate [16], causing the sc-PVDF's to have higher molecular weight. Moreover, higher polydispersities are produced because a reaction equilibrium starting from a higher initial pressure has to experience a greater pressure difference, which is parallel to the change of chain growth rate affecting the size of polymer molecules.

**Tab. 1.** Polymerization of VDF in sc-CO<sub>2</sub> and water emulsion.

Sample	Init.Pres. MPa	Init. Tem. °C	[I] mmol/L	[M] mol/L	Mn ×10 <sup>-4</sup>	Mw ×10 <sup>-4</sup>	Mw/Mn	Yield wt%	H-H defect mol %
sc-1	10.5	60	3.03	3.13	6.5	9.1	1.41	6.5	3.99
sc-2	26	55	3.03	4.38	24.4	40.5	1.66	10.5	3.67
sc-3	26.5	55	3.83	5.63	21.8	39.7	1.82	7.5	4.35
sc-4	27	55	4.18	5.31	13.4	31.7	2.38	14.3	4.38
sc-5	27.5	55	5.15	3.13	11.7	23.4	2.01	11.2	4.16
sc-6	24.5	55	5.22	3.13	12.7	22.8	1.79	7.5	4.03
sc-7	26.8	60	7.71	3.13	14.9	29.0	1.95	80	4.31
sc-8	28	60	15.6	5.47	3.3	5.2	1.56	27.2	3.73
o-PVDF					12.8	72.3	5.65		5.60

In Table 1, both sc-7 and sc-8 show much higher reaction conversions. The reason being possibly the drastic exothermal effect owing to a great amount of initiator leading to the increase of the reaction pressure for a short time, then the increase of polymerization rate; hence, more VDF monomers has to be consumed in order to reach the new reaction equilibrium.

#### -H-H defect concentration of sc-PVDFs

The H-H defect concentration can be determined using <sup>19</sup>F NMR [31]. The <sup>19</sup>F NMR spectrum of the peak assignments of a sc-PVDF are shown in Figure 1. The chemical shifts at -103 ppm (peaks F), -107.3 ppm (very weak) were attributed to the end groups [32-35]. The H-H defect units appear at the chemical shifts -113 ppm and 116 ppm (peaks D and E in Figure 1). The H-H defect concentrations of typical commercial PVDF varies 3~6% [14]. The value of the sc-PVDFs are about 4.0%, and that of ordinary PVDF (o-PVDF) obtained from the emulsion polymerization is 5.6% (Table 1).

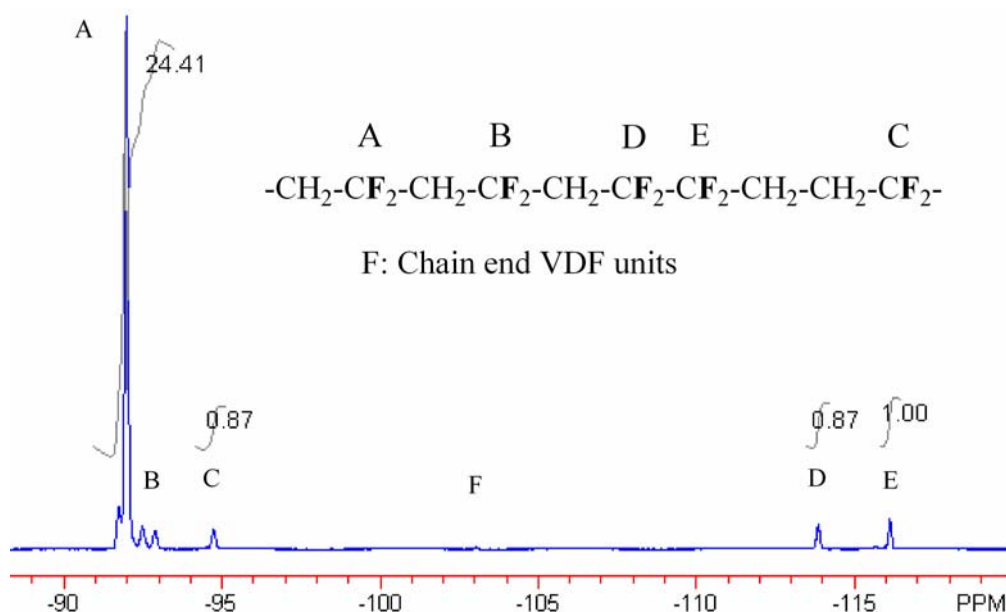


**Fig. 1.**  $^{19}\text{F}$  NMR spectrum of sc-8 ( $\text{d}_6$ -DMSO, 400 MHz).

#### -Effect of Pressure on Morphology of sc-PVDFs

The special features of sc- $\text{CO}_2$  polymerizations are investigated through the morphology of products under SEM. The morphology and the initial pressure of all products are listed in Table 2. It is interesting that the sc-PVDFs' micro morphology (Figure 2) changes from particles to porous, even to floc with the increase of the reaction pressure. Generally, the micro morphology of commercial PVDFs obtained by other polymerization techniques is particles. Thus, as shown in Figure 2, supercritical polymerization has provided an easy way to adjust the product morphology, which is useful for the application of the polymers.

**Tab. 2.** Effect of Pressure on Morphology of sc-PVDFs.

entry	sc-1	sc-2	sc-3	sc-4	sc-5	sc-6	Sc-7	sc-8
Init. Press. MPa	10.5	26	26.5	27	27.5	24.5	26.8*	28*
Polymer appearance	fine powder (F. 1A)	Coarse powder (F. 1B)	Coarse powder	Coarse powder	Coarse powder	Coarse powder	coagulated polymer (F. 1C)	fine powder (F. 1D)
SEM images	particles (F. 1E)	porous with particles (F. 1F)	porous with particles	porous with particles	porous with particles	particles	flock (F. 1G)	flock (F. 1H)

\*: the reactions had drastic exothermal effect to cause pressure and temperature rising because of greater amount of initiator concentration.

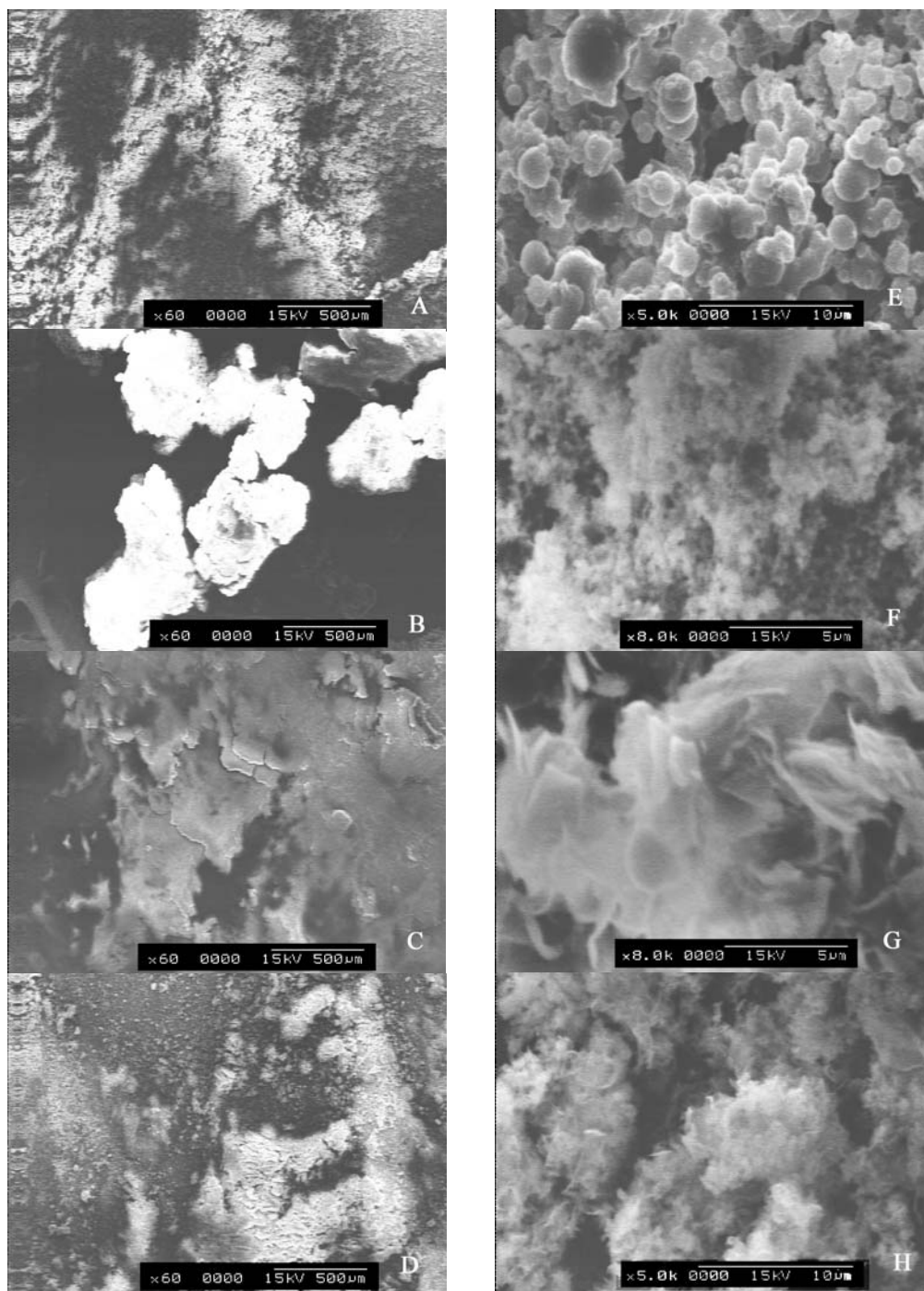


**Fig. 2.** The Morphology of sc-PVDFs. sc-1 (A, E), sc-2 (B, F), sc-7 (C, G), sc-8 (D, H).

Briscoe etc., have proven the elevation of the coefficient of diffusion of carbon dioxide into the polymer with pressure or concentration, and the increase of polymer dilatation and mass sorption with pressure [36]. The polymer molecules form particles under lower pressure (Figure 2 E), the polymer swell and expand to become gradually porous with increasing pressure, (for example, Figure 2 F), and on further increase of pressure, the polymer expand to form cotton-like floc due to exothermal effect (Figure 2 G and H). It is likely that the sc-CO<sub>2</sub> becomes better solvent when pressure increased and influences the morphology of products a lot.



### -Effect of Reaction Pressure on Crystallization

The crystalline properties of the PVDFs determined by DSC are shown in Table 3. It is found that the melting temperatures ( $T_m$ ) increase with the increase of initial pressure. Evidently, the increase of the pressure can induce the PVDF to form more complete (thicker, or crystal phase with higher  $T_m$ ) crystals. Wide-angle X-ray diffraction (WAXRD) intensities (Figure 3) of sc-PVDFs and o-PVDF also demonstrate that the degree of crystallinity of sc-PVDFs increase with reaction pressure (from sc-1 to sc-8). The sample sc-1 has the weakest peak at a bragg angle, 26.6 on Figure 3, its DSC result shows the lowest  $T_m$  among several samples; and the sample sc-8 has the strongest peak at this bragg angle and the highest  $T_m$ .

The possible explain can be proposed as following: The growth of a crystal may involve successive deposition of sequences at the edge of a developing layer; this step has been assumed to be rate controlling on the growth of polymer crystals [37]. Hence, the faster reaction rate generated by higher initial pressure will provide more macromolecule segments in a certain time to deposit in the growing crystal layer, which leads to thicker crystals. At the same time, plasticization by the sc-CO<sub>2</sub> leads to increase in free volume and chain mobility (as shown in Figure 2) [36]. Presumably, the polymer chains could fold more in greater spaces at greater rates. Even the VDF monomers could permeate into the polymer particles and react with the reactive molecular chain ends, then form additional crystal folds.

**Tab. 3.** Initial reaction pressure and property of PVDFs.

Sample	Initial pressure MPa	Crystallinity -1 <sup>a</sup> , f(%)	Tc1 (°C)	β%1	Tm1 (°C)	Crystallinity -2 <sup>b</sup> , f(%)	Tc2 (°C)	β%2	Tm2 (°C)
sc-1	10.5	28.30	60	81.2	134.9	18.66	102.5	52.9	138.4
sc-2	26	32.67	55	72	150.0	20.29	116.7	52.5	146.9
sc-3	26.5	41.94	55	66.0	158.1	30.17	127.2	61.1	155.6
sc-4	27	56.48	55	63.2	162.4	37.51	134.4	56.2	159.1
sc-5	27.5	49.28	55	61.7	166.1	36.06	134.1	50.9	163.1
sc-6	24.5	28.00	55	73.7	147.9	19.85	112.7	67.9	148.8
sc-7	26.8	53.61	65*	59.3	162.4	32.64	128.2	51.6	161.2
sc-8	28	36.87	65 *	52.6	170.8	25.63	140.0	48.4	167.9
o-PVDF		31.68		67.7	155.5	30.35			156.8

1<sup>a</sup>: The crystallinity of the samples directly obtained from reaction, without any treatment, measured by DSC. 2<sup>b</sup>: The crystallinity of the sample, measured by DSC in the same temperature range with 1<sup>a</sup> after the sample recrystallize after complete melting in DSC. \*: The initial reaction temperature is at 60 °C, however, the temperature rose to 65 °C for more than 10 minutes because of exothermal effect.

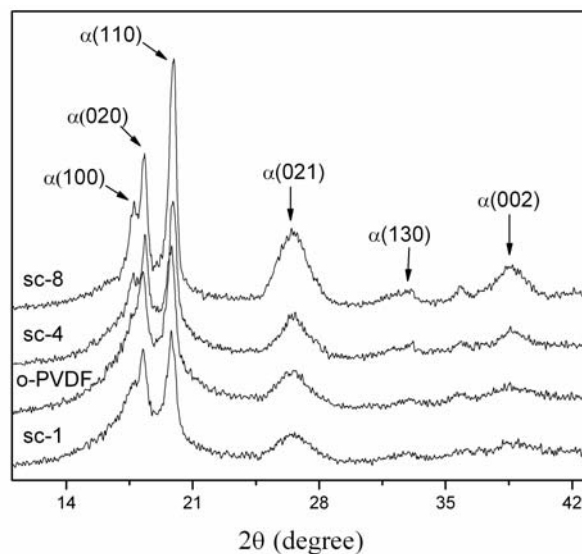


**Fig. 3.** The WAXRD curves of PVDFs.

In addition, sc-CO<sub>2</sub> polymerization has greatly improved the crystallinity of PVDFs. The melting enthalpies of crystal of sc-PVDFs ( $\Delta H_m$ ) were used to calculate their crystallinity by the following equation [38]:

$$X(\%) = (\Delta H_m / \Delta H_{m,c}) \times 100\% \quad (1)$$

Where  $\Delta H_{m,c}$  is the heat of fusion of 100% crystalline polymer. The value for PVDF is 104.7 J/g [39]. Table 3 shows the crystallinity (Crystallinity-1) of the sc-PVDFs before eliminating the heat history and the crystallinity (Crystallinity-2) of the sc-PVDFs recrystallized after eliminating the heat history. Evidently, the sc-PVDF sample directly crystallized in sc-CO<sub>2</sub> has a higher crystallinity, however, it decreases a lot when recrystallized under normal pressure after eliminating the heat history. Table 3 also compares the crystallinity-1 with the crystallinity-2 of o-PVDF obtained from the emulsion polymerization. The results show that two crystallinities of o-PVDF before and after removing the heat history are almost same. Obviously, the crystallization behavior of sc-PVDFs in sc-CO<sub>2</sub> is unique.

#### -Effect of Reaction Pressure and Temperature on Crystalline Phases

The reaction pressure influences the amount of different crystal phases of sc-PVDFs. Figure 4 is FTIR curve of several PVDFs. The peak height ratios between 845 ( $\beta$ ) and 796 ( $\alpha$ )  $\text{cm}^{-1}$ , or 510 ( $\beta$ ) and 530 ( $\alpha$ )  $\text{cm}^{-1}$  decrease from sc-1 to sc-8. It means the decrease of  $\beta$  phase crystals and the increase of  $\alpha$  phase crystals of sc-PVDFs with the increase of initial reaction pressure. Figure 3 shows the significant amount of  $\alpha$  crystal phases of PVDFs by WAXRD [19, 21, 24], however, it is usually difficult to separate pronounced features resulting from *trans* sequence in the  $\beta$  or  $\gamma$  crystalline phases by WAXRD [40, 41]. Thus, Figure 3 can't be used to compare the amount of different crystalline phases. Furthermore, the amount of crystalline phases of PVDF was calculated using DSC curve analysis [21]. During the first heating round, a small melting peak of incomplete crystal was observed in the DSC trace, but it disappeared in the second round of the DSC heating process.

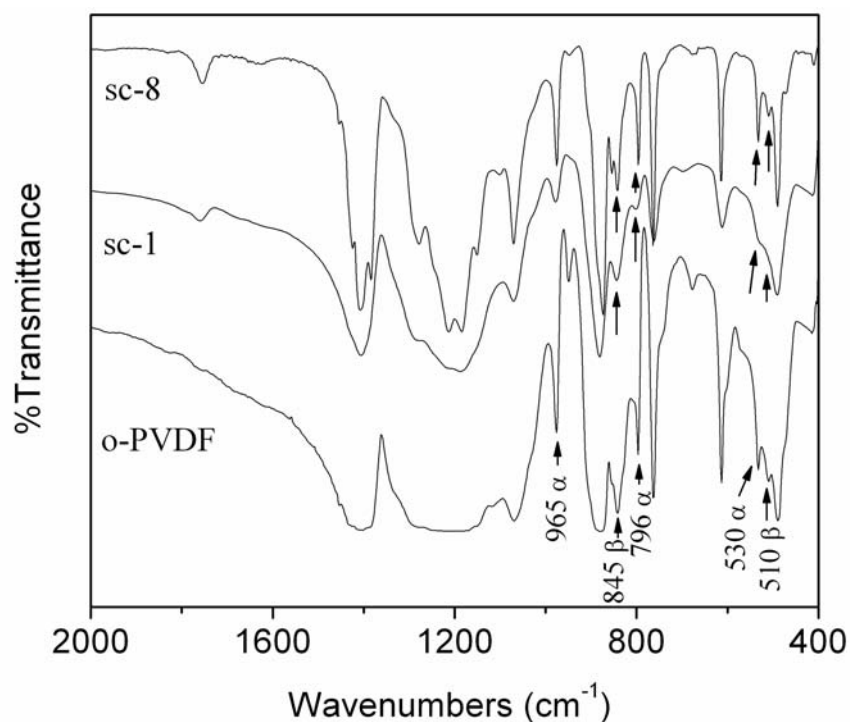


**Fig. 4.** The FT-IR curves of PVDFs.

The small peak should be assigned to  $\beta$  crystalline phase (Figure 5). The crystalline phase percentage was calculated by splitting the peaks of the DSC curves of PVDFs (Figure 6), the results are listed in Table 3.

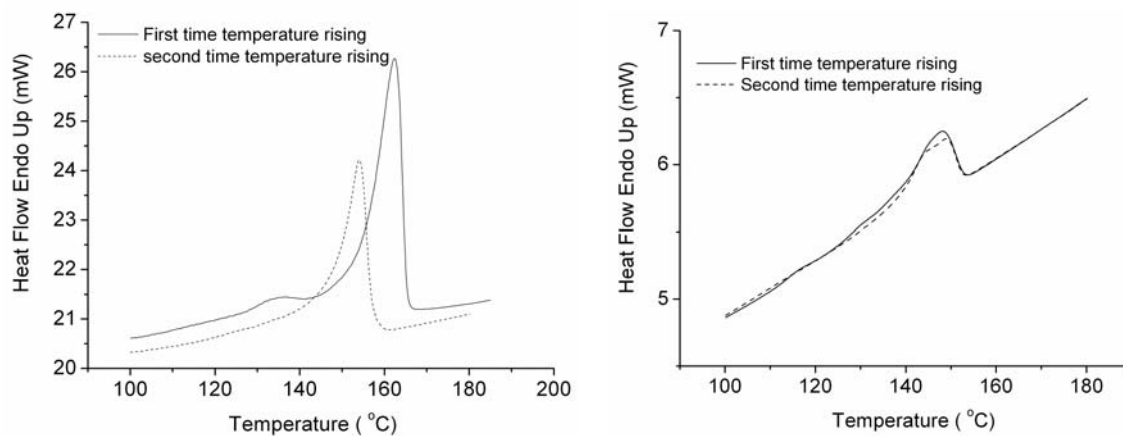


**Fig. 5.** The DSC curves of sc-PVDFs.



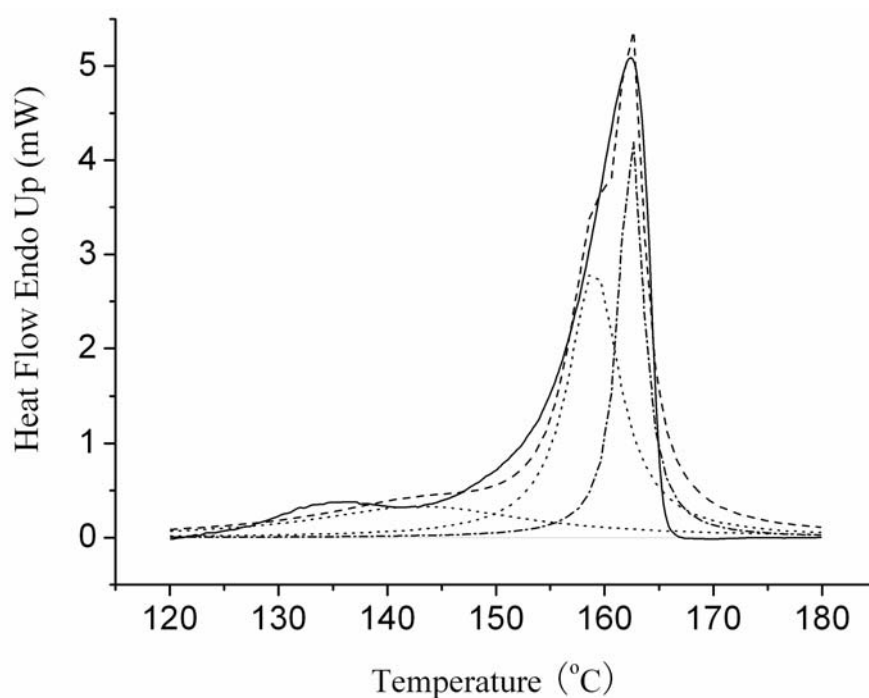


**Fig. 6.** Splitting the DSC peak of sc-4 using Lorentzian fit. Experimental curve (solid line), calculated curve (dash line), calculated individual peak due to the  $\beta$  (dot line) and  $\alpha$  (dash-dot line) phase.

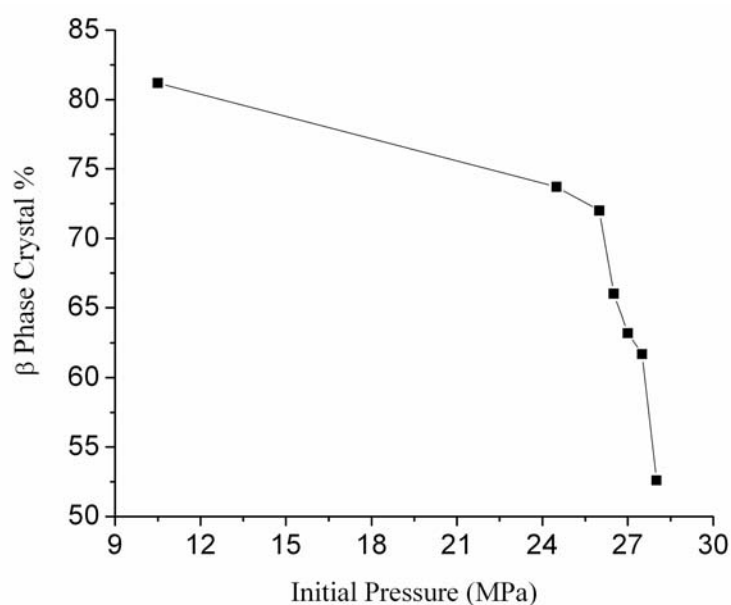


**Fig. 7.**  $\beta$  phase crystal % of sc-PVDFs as a function of initial reaction pressure.

The  $\beta$  crystalline phase percentages of sc-PVDFs polymerized under different reaction pressure were compared in Figure 7. Perhaps, the lower reaction pressure has contributed a lot for the higher  $\beta$  phase crystal concentration of sc-PVDFs. It is

speculated that the more  $\beta$  phase crystal forms when the PVDF is generated in sc-CO<sub>2</sub> under lower pressure. The  $\beta$  crystalline phase of PVDF is very useful due to its special piezo- and pyro-properties [3]. Therefore, sc-CO<sub>2</sub> polymerization might be utilized to obtain the PVDF with a great amount of  $\beta$  crystalline phase under suitable polymerization conditions.

It was also found that the content of  $\alpha$  phase is less than  $\beta$  phase in the crystals of the sc-PVDFs, however, the content of  $\alpha$  phase increases when the PVDFs are recrystallized in DSC oven after removing their heat history at 185 °C. Gregorio, Jr. and Cestari have reported the fraction of  $\beta$  phase of PVDFs reduces from 1.0 at 40 °C to 0.0 at 160 °C, and the fraction of  $\alpha$  phase increases from 0.0 at 60 °C to maximal value, 1.0, at 130 °C [20].

We found that the sc-8 has the highest  $\alpha$  phase crystalline content for its highest reaction temperature reach 65 °C, and sc-2, 4, 6 whose reaction temperatures were controlled at 55 °C crystallize into more  $\beta$  phase crystals. The results are in agreement with the report of Gregorio et al. In addition, although the sc-PVDFs recrystallize at a temperature of more than 100 °C under normal pressure, the amount of  $\beta$  crystal phase of sc-PVDFs is maintained quite high (see “ $\beta\%$ 2” shown in Table 2). Figure 8 is the DSC melting curve of the sc-8 recrystallized under normal pressure.

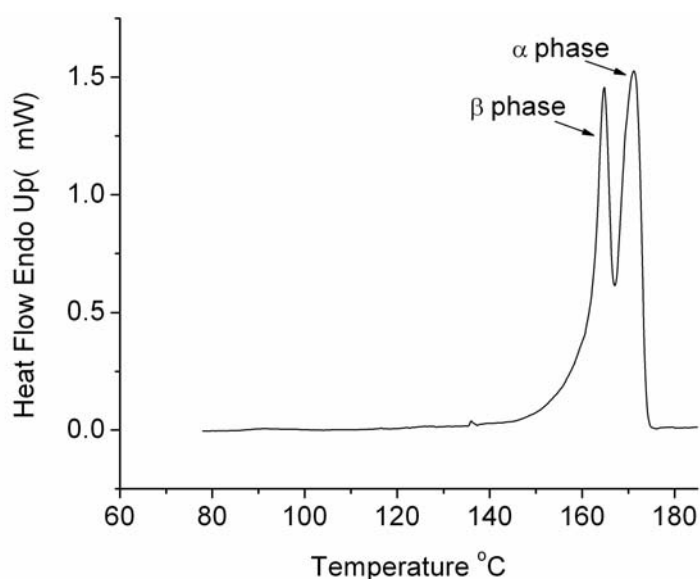


**Fig. 8.** DSC curve of sc-8 recrystallized at 140 °C after completely melting at 185 °C.

#### -Effect of Reaction Pressure on Crystallinity of PVDFs

The polydispersity of polymers increases with the reaction pressure, and sc-CO<sub>2</sub> can affect the crystallinity of polymers. Table 3 presents some results about the effect of the reaction pressure on polymers' crystallinity. Figure 9 (1 for crystallinity-1) also shows that the crystallinity of PVDFs obtained from sc-CO<sub>2</sub> increases with the broadening molecular weight distribution of the polymers. It is possible that the increase of reaction pressure in sc-CO<sub>2</sub> could increase the crystallinity of polymers.

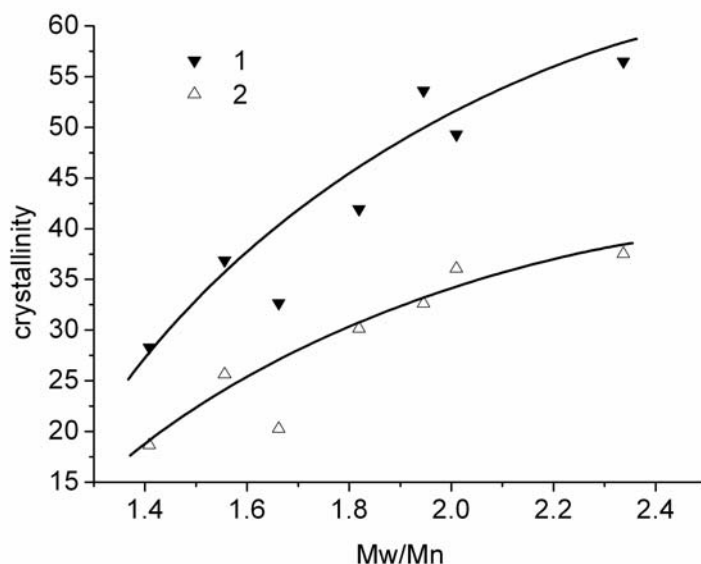


**Fig. 9.** Crystallinity of sc-PVDFs as a function of MWD ( $M_w/M_n$ ). **1, 2** : the crystallinity before and after removing the heat history of sc-PVDFs, respectively.

#### -Effect of H-H Defect Concentration on Crystallization of sc-PVDFs

The crystallinity of sc-PVDFs, recrystallized under normal pressure after removing their heat history, apparently increase with the increasing molecular weight distribution (Figure 9, **2** for crystallinity-2). This phenomenon has also been observed from the crystallization of the polypropylene at given spinning conditions [42]. It can be explained by the nucleation mechanism of polymer crystallization: Smaller molecules firstly crystallize due to the weak interaction among molecules, and then the small crystals supply the nucleating agents for the crystallization of greater molecules.

Sc-4, sc-5 and o-PVDF have a similar molecular weight, but the molecular weight distribution of the o-PVDF is much wider (Table 1). Hence, the o-PVDF should have a higher crystallinity. In fact, the crystallinity of o-PVDF is relatively lower. We speculate that some other features of sc-PVDFs still influence the crystallization of polymers under normal conditions. Nandi and Mandelkern found that the crystallinity of PVDF decreases with the increase of the H-H defect concentration of PVDF [22]. The possible reason is that the H-H defect concentration of the o-PVDF is higher than those of the sc-PVDFs, so the greater defect structure decreases the regular repetition of monomer units of the chains to cause more terminations of crystallization. Therefore, although the sc-PVDFs have narrower molecular weight distributions, they possess higher crystallinity for their lower H-H defect concentrations. This will be favorable to improve the mechanical property of PVDF.

#### Conclusions

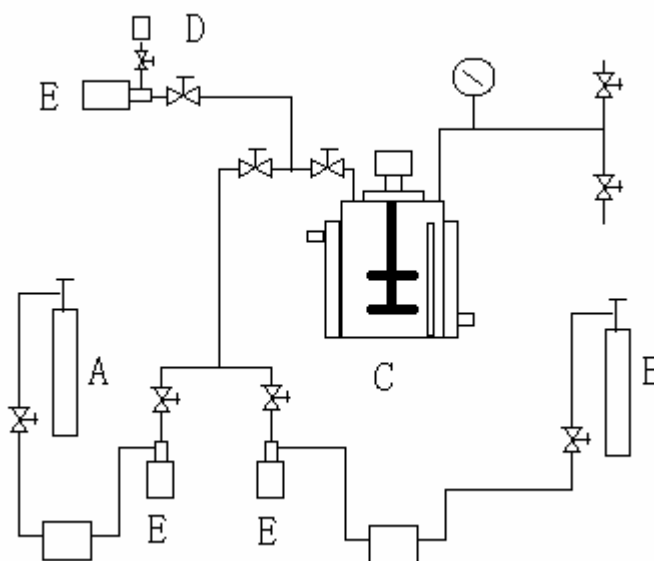
The sc- $\text{CO}_2$  polymerization influences morphology, molecular weights, polydispersities and H-H defect concentrations of obtained PVDFs. During polymerization, the great pressure and good solubility of sc- $\text{CO}_2$  improve the complete degree of crystallinity, crystallinity, and affect crystalline phases of PVDFs, which shows a unique effect of sc- $\text{CO}_2$  polymerization on PVDF's crystallization. The sc- $\text{CO}_2$  polymerization promises well for obtaining the PVDF with better physical properties and application.

## Experimental Part

### Materials

Vinylidene fluoride monomer and initiator diisopropyl peroxydicarbonate were generously donated by Shanghai 3F new material Co., Ltd (Shanghai, China) and used without further purification. Carbon dioxide (Pure degree: 99.995%) was supplied by Shanghai Chenggong gas Co., Ltd (Shanghai, China). Initiator was dissolved in CFC-113 (Supplied by Shanghai Wulian Chemical Factory, China) (52 wt % wrt CFC-113).

### Polymerizations



**Scheme 1.** The sc-CO<sub>2</sub> polymerization apparatus. A: Monomer cylinder; B: CO<sub>2</sub> cylinder; C: Autoclave; D: Initiator solution funnel; E: Syringe Pumps.

PVDF polymerized in sc-CO<sub>2</sub> (sc-PVDF): Scheme 1 provides a sketching of the experimental polymerization apparatus. This equipment and the associated synthetic procedure were similar to that described elsewhere [12-16, 27, 28]. The polymerizations were carried out in a 1.0 L stainless steel autoclave. A typical procedure was as following: The autoclave was sealed and leak-tested with carbon dioxide. After releasing CO<sub>2</sub>, the autoclave and pipes were purged with CO<sub>2</sub> and VDF for several minutes. VDF of a weight determined by an electronic balance under VDF Cylinder (A in Scheme 1) was condensed with freezing machine into the sc-PVDF tank and pumped into the autoclave. Carbon dioxide (Cylinder B in Scheme 1) was condensed, and then pumped into the autoclave until the pressure in the autoclave reached 7.0 MPa at room temperature, then the reaction autoclave was agitated at 300 rpm and heated to the reaction temperature (55 °C, except sc-1, sc-7 and sc-8 which is at 60 °C). Additional carbon dioxide was added to the autoclave until the pressure reached 27 MPa at reaction temperature. Finally, the initiator solution was directly pumped into the autoclave through a funnel at 27 MPa in a time less than a minute. Once the reaction pressure changed (the reaction pressures and

temperatures of sc-7 and sc-8 with higher initiator concentrations increased, but the reaction temperatures of other sc-PVDFs kept stable and their reaction pressures lowered), the reaction was thought to begin. After two hours, the heating and agitation were stopped, and then the CO<sub>2</sub> was vented slowly in 20 minutes in order to avoid a blocking of the vent connection (during the time, the polymerization may continue). At the end, the autoclave was opened and the polymer was collected and weighted.

Ordinary PVDF (o-PVDF) obtained by emulsion polymerization: A water emulsion method was employed to obtain the product at 60 °C, under 3.0 MPa pressure. Initiator was diisopropyl peroxydicarbonate. The products were washed with hot water for several times to purify.

### Analysis

Gel permeation chromatography (GPC) of sc-PVDFs was performed at 70 °C using a Perkin Elmer Series-200 system with PL gel (10 µm) 300 mm × 7.5 mm mixed-B columns and N, N-dimethylformamide (DMF) modified with 0.1 M LiBr as the solvent and using a PE pump (series 200), a refractive index detector (series 200). The GPC was calibrated at 70 °C using molecular weight distribution standards of polystyrene (PS). The sc-PVDF concentration in DMF is 1.5 g/L, 100 µL of which is injected into sc-PVDF loop and flows at 1.0 mL/min in the columns.

The crystallinity of PVDF was determined using a Perkin Elmer Pyris-1 DSC at a temperature-rising rate of 10 K/min. The scanning temperature ranged from 323 K~473 K. Two cycles of temperature rising were carried out for the PVDFs.

Wide-angle X-ray diffraction (WAXRD) measurements were performed using a XRD-6000 X-ray diffractometer (SHIMADZU) with Cu target (40Kv, 30mA,  $\lambda=1.5406 \text{ \AA}$ ) on specimens of about 1mm thickness, and the scanning rate was 4°/min.

The sequence structure of the PVDFs was characterized by <sup>19</sup>F NMR which was performed on Bruker av400 spectrometer using DMSO-*d*<sub>6</sub> as the solvent at 20 °C.

The fourier transform infrared spectroscopy (FT-IR) was taken with a Perkin Elmer Paragon 1000 FT-IR spectrometer. The data of 100 scans were averaged.

The morphology of the PVDF product was determined using a Hitachi S-2150 scanning electronic microscope (SEM) machine. The sample was mounted on an aluminium stub using an adhesive carbon tab and gold coated before images were obtained.

### Acknowledgements

The research was supported in parts by the Shanghai 3f New Material Co., Ltd., China. We thank them for contributing experimental equipments and materials, as well as some analysis tests.

### References

- [1] Zhang F. X.; *Modern Piezoelectrics* Beijing: Science Publishing Company, China, **2002**, p. 239~240.
- [2] Lu F. J.; Hsu, S. L.; *Macromolecules* **1986**, *19*, 326-329.
- [3] Lovinger A. J.; *Macromolecules* **1981**, *14*, 322-325.
- [4] Klinge U.; Klosterhalfen B.; Ottinger A. P.; Junge K.; Schumpelick V.; *Biomaterials* **2002**, *23*, 3487-3493.

- [5] Dohaney J. E.; Humphery J. S.; *In Encyclopedia of Polymer Science and Engineering* Mark H. F.; Bilkales N. M.; Overberger C. G.; Menges G.; Eds.; Wiley: New York, **1989**, Vol. 17.
- [6] Russo S.; Pianca M.; Moggi G.; *In Poly(vinylidene fluoride)* Salamone J. C.; Ed.; CRC: Boca Raton F. L.; **1996**, Vol.9.
- [7] Darr J. A.; Poliakoff M.; *Chem. Rev.* **1999**, 99, 495-541.
- [8] Vesovic V.; Wakehan W. A.; Olchow G. A.; Sangers J. V.; Watson J. T. R.; Millat J.; *J. Phys. Chem. Ref. Data*, **1990**, 19, 763-808.
- [9] Plesch P. H.; Biddulph R. H.; *J. Chem. Soc.* **1960**, 82, 3913.
- [10] Kendall J. L.; Canelas D. A.; Young J. L.; DeSimone J. M.; *Chem. Rev.* **1999**, 99, 543-563.
- [11] Desimone J. M.; Guan Z.; Elsbernd C. S.; *Science* **1992**, 257, 945-947.
- [12] Charpentier P. A.; DeSimone J. M.; Robrets G. W.; *Ind. Eng. Chem. Res.* **2000**, 39, 4588-4596.
- [13] Saraf M. K.; Gerard S.; Wojcinshi II L. M.; Charpentier P. A.; DeSimone J. M. and Robrets G. W.; *Macromolecules* **2002**, 35, 7976-7985.
- [14] Tai H. Y.; Wang W. X.; Martin R.; Liu J.; Lester E.; Licence P.; Woods H. M.; Howdle S. M.; *Macromolecules* **2005**, 38, 355-363.
- [15] Tai H. Y.; Wang W. X.; Howdle M. S.; *Macromolecules* **2005**, 38, 1542-1545.
- [16] Tai H. Y.; Wang W. X.; Howdle M. S.; *Polymer* **2005**, 46, 10626-10636.
- [17] Lovinger A. J.; *Macromolecules* **1982**, 15, 40-44.
- [18] Naegele D.; Yoon D.Y.; Broadhurst M. G.; *Macromolecules* **1978**, 11 (6), 1297-1298.
- [19] Yasuhiro T.; Yoshiaki M.; Hiroyuki T.; *Macromolecules* **1982**, 15, 334-338.
- [20] Gregorio Jr. R.; Cestari M.; *J. Polym. Sci: Part B: Polym. Phys.* **1994**, 32, 859-870.
- [21] Laroche G.; Lafrance C. P.; Prud'homme R. E.; Guidoin R.; *J. Biomed. Mater. Res.* **1998**, 39, 184-189.
- [22] Nandi A. K.; Mandelkern L.; *J. Polym. Sci.: Polym. Phys.* **1991**, 29, 1287~1297.
- [23] Takeshi H.; Masamichi H.; Ohigashi H.; *Polymer* **1996**, 37, 85~91.
- [24] Gorlitz M.; Minke R.; Trautvetter W.; Weisgerber G.; *Angew. Makromol. Chem.* **1973**, 29/30, 137-162.
- [25] Butler G. B.; Olson KG; and Tu C. L.; *Macromolecules* **1984**, 17, 1887-1889.
- [26] Herman; Toshiyuki U.; Astushi K.; Susumu U.; *Polymer*, **1997**, 38, 1677-1683.
- [27] Saraf M. K.; Wojcinski L. M.; Kennedy K. A.; *Macromol. Symp.* **2002**, 182, 119-29.
- [28] Liu J.; Tai H. Y.; Howdle M. S.; *Polymer*, **2005**, 46, 1467-1472.
- [29] Van E. R.; Asano T.; Noble W. J. L.; *Chem. Rev.* **1989**, 89, 549.
- [30] Hutchenson K. W.; *In Supercritical Fluid Technology in Materials Science and Engineering* Sun Y. P. Ed, New York: Marcel Dekker, **2002**. p. 87-187.
- [31] René S. L.; Bruno A.; *J. Fluorine Chem.* **2002**, 116, 27-34.
- [32] Pianca M.; Barchiesi E.; Esposto G.; Radice S.; *J. Fluor. Chem.* **1999**, 95, 71-84.
- [33] Ameduri J.; Guiot, B.; Boutevin B.; *Macromolecules* **2002**, 35, 8694-8707.
- [34] Cais R. E.; Kometani J. M.; *Macromolecules* **1985**, 18, 1357-1359.
- [35] Russo S.; Behari K.; Shan C. J.; *Polymer* **1993**, 34, 4777-4781.
- [36] Briscoe B. J.; Lorgy O.; Wajs A.; Dang P.; *J. Polym. Sci. B: Polym. Phys.* **1998**, 36, 2435-2447.
- [37] Flory P. J.; *J. Am. Chem. Soc.* **1962**, 84, 2857-2866.
- [38] Lin S. A., Lu Y.; *Polymer Chemistry* Beijing: Science Publishing Company, China, **2000**, p. 36-39.



- [39] Wang Y. D.; Cakmak M.; *J. Appl. Polym. Sci.* **1998**, 68, 909–926.
- [40] Lee W. K.; Ha C. S.; *Polymer* **1998**, 39(26), 7131-7134.
- [41] Yang D. Y.; Tomas E. L.; *J. Mater. Sci. Lett.* **1984**, 3, 929.
- [42] Misra S.; Lu F.-M.; Spruiell J. E.; Richeson G. C.; *J. Appl. Polym. Sci.* **1995**, 56(13), 1761-1779.